IEEE Access
Multidisciplinary | Rapid Review | Open Access Journal

Received August 23, 2021, accepted September 20, 2021, date of publication September 27, 2021, date of current version October 6, 2021.

Digital Object Identifier 10.1109/ACCESS.2021.3115782

An Improved Model-Free Current Predictive Control Method for SPMSM Drives

XUERONG LI[1], YANG WANG[2], XINGZHONG GUO[1], XING CUI[2], SHUO ZHANG[1], (Member, IEEE), AND YONGSHEN LI[3], (Graduate Student Member, IEEE)

[1]Key Laboratory of Advanced Perception and Intelligent Control of High-end Equipment, Ministry of Education, Anhui Polytechnic University, Anhui 241000, China
[2]North Vehicle Research Institute, Beijing 100072, China
[3]National Engineering Laboratory for Electric Vehicles, School of Mechanical Engineering, Beijing Institute of Technology, Beijing 100081, China

Corresponding author: Shuo Zhang (shuozhangxd@gmail.com)

This work was supported in part by the Key Areas of Guangdong Province through the Project "Integration and Industrialization of High Performance, Long Endurance, and Integrated Electric Drive System" under Grant 2019B090910001, and in part by the Key Laboratory of Advanced Perception and Intelligent Control of High-End Equipment, Ministry of Education Open Topic, under Grant GDSC202008.

ABSTRACT Traditional model predictive current control (MPCC) method depends on motor model for predictive control, when the motor parameters change with the working conditions, the predictive performance of MPCC will be deteriorated. To improve the parameter robustness of MPCC, a model-free current predictive control method that combines ultra-local model and sliding mode observer is proposed. First, the prediction model of MPCC based on the mathematical model of surface-mounted permanent magnet synchronous motor (SPMSM) is replaced by the ultra-local model that does not use any motor parameters. Second, the sliding mode observer is adopted to observe the parameter of ultra-local model and compensate parameter disturbance. Finally, the stability of the sliding mode observer is proved by the Lyapunov stability criterion. The traditional MPCC method and the proposed model-free current predictive control method are comparatively analyzed, simulation and experimental results show that the proposed model-free current predictive control method can improve the parameter robustness of MPCC.

INDEX TERMS Model-free predictive control, parameter robustness, surface-mounted permanent magnet synchronous machine.

I. INTRODUCTION

In recent years, surface-mounted permanent magnet synchronous motor (SPMSM) has attracted more attention in the field of electric vehicle drive systems because of its advantages of high power density and high efficiency [1].

A. LITERATURE REVIEW

The control strategies used in the SPMSM's drive systems mainly include field-oriented control (FOC), direct torque control (DTC) and model predictive control (MPC) [2]–[5]. Among them, FOC is the most commonly used control strategy, which controls flux linkage and electromagnetic torque directly by decoupling stator current to *dq* rotating coordinate system. While the proportion parameter and integration parameter of PI regulator in FOC need to be adjusted empirically [2]. DTC takes flux linkage and electromagnetic torque as control targets directly, with the advantages of fast torque response and strong robustness. While the torque ripple and current ripple are high because of the limited number of effective voltage vectors. Besides, the switching frequency of DTC is not fixed [3], [4].

MPC has been used widely for its advantages of high dynamic performance, multivariable constraint and clear physical concept [5]. MPC needs a prediction model to describe dynamic behavior and predicts future information based on present and historical information. In the field of motor drive systems, MPC uses the mathematical model of motor for predictive control. MPC method can be divided into finite control set model predictive control (FCS-MPC) method and continuous control set model predictive control(CCS-MPC) method according to the number of output vectors [6]. FCS-MPC obtains the optimal effective voltage vector through enumeration method which needs

The associate editor coordinating the review of this manuscript and approving it for publication was Madhav Manjrekar.

large computation [7]. In addition, FCS-MPC has no modulation module, the finite number of voltage vector makes large current ripple and torque ripple in the steady state [8]. CCS-MPC combines modulation module, the optimal voltage vector can be obtained through modulator, and the switching frequency is fixed [9].

MPC requires accurate motor model and motor parameters for predictive control. If the motor parameters have measurement error or change with the working conditions, the predictive performance of MPC will be greatly destroyed, resulting in a negative impact on the motor drive system eventually [10].

To improve the parameter robustness of MPC, different solutions have been proposed. Reference [11] proposed a robust high bandwidth discrete-time predictive current control method. While this method needs large computation, which can present an additional system delay. Reference [12] proposed a neural networks-based adaptive dynamic surface control method to increase the parameter robustness. While this method is quite complex. Reference [13] proposed an online parameter identification method based on reference model. While this method is time-consuming.

Disturbance observer methods can achieve parameter robust control to PMSM by observing and compensating current disturbance caused by parameters mismatch [14]. Reference [15] proposed a Luenberger disturbance observer method which could observe the system disturbance and compensate the disturbance in real time. While it requires a linear controlled object and needs more given information of the control system. Reference [16] proposed a method that used a non-linear disturbance observer to enhance the prediction accuracy under parameter mismatch. Reference [17] proposed a method that combined the extended state observer(ESO) and dead-beat current predictive control method, which improved the parameter robustness of the control system, while this method has a complex structure and involves many adjusted parameters. To reduce the complexity, reference [18] proposed a sliding-mode disturbance observer method. Which could predict stator current and compensate current disturbance caused by parameter mismatch.

In addition to the methods with disturbance observer, reference [19] proposed a model-free control method which has been widely concerned in the field of intelligent transportation. The main characteristic of model-free control method is that it does not need any motor parameter. Reference [20] proposed a model-free predictive control method based on FCS-MPC. While the stator current needs to be sampled twice in each control cycle, which brings current peak and affects the controller performance. To solve the problem of current peak, reference [21] presented an improved model-free control method. In this method, the second current sampling was delayed for a fixed time. However, due to the dependence on the characteristics of the controller, it is difficult to determine the specific delay time. Besides, there exists a current difference update stagnation problem in this method. A model-free predictive control method was proposed to solve the problem of current difference update stagnation in reference [22]. But this method would increase the current ripple as the system was forced to apply a sub-optimal even worst switching state. Reference [23], [24] presented an innovative method that combined ultra-local model with deadbeat current predictive control method to solve the parameters uncertainty problem. However, the tuning process of this method is complex, and the control performance will decline under a relatively low sampling frequency [25]. Reference [25] proposed a method that combined ultra-local model with extended state observer, which has fewer adjusted parameters. However, complexity structure and delay of the control system would result in unsatisfactory performance.

B. MOTIVATION AND INNOVATION

Parameter disturbance is an urgent problem to be solved in the MPC strategy. To improve the parameter robustness of the SPMSM drive system, this paper proposes an improved model-free current predictive control method. The proposed method combines the ultra-local model with the sliding mode observer. The complexity of the designed sliding mode observer is less than ESO, which reduces the calculation burden. The main significance of this paper can be described as follows:

1) This paper adopts single input single output ultra-local model of SPMSM for current predictive control. The ultra-local model of SPMSM takes voltage vector as input variable and the derivative of stator current as output variable.
2) The sliding mode observer based on exponential approach law is adopted to estimate and compensate the current disturbance caused by parameter disturbance. The designed observer is simple, improves the accuracy of current prediction and reduces calculation burden of the control system.
3) Simulation and experimental results demonstrate the parameter robustness of the improved model-free current predictive control method.

C. PAPER ORGANIZATION

The writing framework of this paper can be described as follows. Section II introduces the mathematical model of SPMSM and the working mechanism of CCS-MPC. Section III presents the mechanism of traditional model-free predictive control method. The ultra-local model and the sliding mode observer are introduced first in section IV, then elaborates the theoretical analysis of the improved model-free current predictive control method and proves the stability of the designed controller. Simulation results and experimental results are shown in section V and section VI respectively.

II. CONTINUOUS CONTROL SET MODEL PREDICTIVE CURRENT CONTROL

The CCS-MPC method has infinite voltage vectors to be chosen, so it can track the reference current value precisely.

In this paper, the research object is three-phase surface-mounted permanent magnet synchronous motor (SPMSM).

In order to understand CCS-MPC method better, the mathematical model of SPMSM is introduced first, and then the mechanism of CCS-MPC method is described.

A. THE MATHEMATICAL MODEL OF SPMSM

After ignoring some minor factors and conducting coordinate transformation, the mathematical model of SPMSM in the two-phase rotation coordinate system can be expressed as follows.

$$\begin{aligned} u_{\mathrm{d}} &= R_{\mathrm{s}} i_{\mathrm{d}} + L_{\mathrm{s}} \frac{di_{\mathrm{d}}}{dt} - w_{\mathrm{e}} L_{\mathrm{s}} i_{\mathrm{q}} \\ u_{\mathrm{q}} &= R_{\mathrm{s}} i_{\mathrm{q}} + L_{\mathrm{s}} \frac{di_{\mathrm{q}}}{dt} + w_{\mathrm{e}} L_{\mathrm{s}} i_{\mathrm{d}} + w_{\mathrm{e}} \psi_{\mathrm{f}} \\ T_{\mathrm{e}} &= 1.5 p \psi_{\mathrm{f}} i_{\mathrm{q}} \\ T_{\mathrm{e}} - T_{\mathrm{l}} &= J \frac{dw_{\mathrm{m}}}{dt} \end{aligned} \tag{1}$$

In the equation, u_{d} represents the d-axis voltage, and u_{q} represents the q-axis voltage, R_{s} is stator resistance, L_{s} is stator inductance and Ψ_{f} is rotor flux linkage, w_{e} denotes the electrical angular velosity, w_{m} denotes the mechanical angular speed, T_{e} represents the electromagnetic torque and T_{l} represents load torque, p denotes the number of pole pairs, J denotes the machine inertia.

B. THE MECHANISM OF CCS-MPC

The CCS-MPC method adds Space Vector Pulse Width Modulation (SVPWM) module to synthesize the reference voltage vector by using the basic voltage vectors.

Assuming the sampling period of the control system is T_{s}, the current predictive model of SPMSM in the rotor rotation coordinate system by using first-order Euler equation is described in (2). Assuming the present time is k,

$$\begin{aligned} i_{\mathrm{d}}(\mathrm{k}+1) &= i_{\mathrm{d}}(\mathrm{k}) + \frac{T_{\mathrm{s}}}{L_{\mathrm{s}}}[u_{\mathrm{d}}(\mathrm{k}) - R_{\mathrm{s}} i_{\mathrm{d}}(\mathrm{k}) + L_{\mathrm{s}} w_{\mathrm{e}}(\mathrm{k}) i_{\mathrm{q}}(\mathrm{k})] \\ i_{\mathrm{q}}(\mathrm{k}+1) &= i_{\mathrm{q}}(\mathrm{k}) + \frac{T_{\mathrm{s}}}{L_{\mathrm{s}}}[u_{\mathrm{q}}(\mathrm{k}) - R_{\mathrm{s}} i_{\mathrm{q}}(\mathrm{k}) - L_{\mathrm{s}} w_{\mathrm{e}}(\mathrm{k}) i_{\mathrm{d}}(\mathrm{k}) \\ &\quad - w_{\mathrm{e}}(\mathrm{k}) \psi_{\mathrm{f}}] \end{aligned} \tag{2}$$

where $i_{\mathrm{d}}(\mathrm{k})$ and $i_{\mathrm{q}}(\mathrm{k})$ denote the sampling stator currents at time k, $i_{\mathrm{d}}(\mathrm{k}+1)$ and $i_{\mathrm{q}}(\mathrm{k}+1)$ denote the predictive stator currents at time $\mathrm{k}+1$.

In the actual experimental system, the switching frequency of inverter is 20 kHz, which is much faster than the variation of the stator reference current. Therefore, the stator reference current at time $\mathrm{k}+1$ can be considered as equal to the stator reference current.

$$\begin{aligned} i_{\mathrm{d}}^{\mathrm{ref}}(\mathrm{k}+1) &= i_{\mathrm{d}}^{\mathrm{ref}} \\ i_{\mathrm{q}}^{\mathrm{ref}}(\mathrm{k}+1) &= i_{\mathrm{q}}^{\mathrm{ref}} \end{aligned} \tag{3}$$

The CCS-MPC contains the modulation module, for the sake of tracking the reference current value, simply replace $i_{\mathrm{d}}(\mathrm{k}+1)$ and $i_{\mathrm{q}}(\mathrm{k}+1)$ in (2) with reference currents $i_{\mathrm{d}}^{\mathrm{ref}}$ and $i_{\mathrm{q}}^{\mathrm{ref}}$ respectively. Then the required optimal voltage can be obtained according to the current predictive model.

$$\begin{aligned} u_{\mathrm{d}}(\mathrm{k}) &= \frac{i_{\mathrm{d}}^{\mathrm{ref}} - i_{\mathrm{d}}(\mathrm{k})}{T_{\mathrm{s}}} L_{\mathrm{s}} + R_{\mathrm{s}} i_{\mathrm{d}}(\mathrm{k}) - L_{\mathrm{s}} w_{\mathrm{e}}(\mathrm{k}) i_{\mathrm{q}}(\mathrm{k}) \\ u_{\mathrm{q}}(\mathrm{k}) &= \frac{i_{\mathrm{q}}^{\mathrm{ref}} - i_{\mathrm{q}}(\mathrm{k})}{T_{\mathrm{s}}} L_{\mathrm{s}} + R_{\mathrm{s}} i_{\mathrm{q}}(\mathrm{k}) + L_{\mathrm{s}} w_{\mathrm{e}}(\mathrm{k}) i_{\mathrm{d}}(\mathrm{k}) + w_{\mathrm{e}}(\mathrm{k}) \psi_{\mathrm{f}} \end{aligned} \tag{4}$$

The CCS-MPC method structure diagram of SPMSM drive systems is shown in the Figure 1.

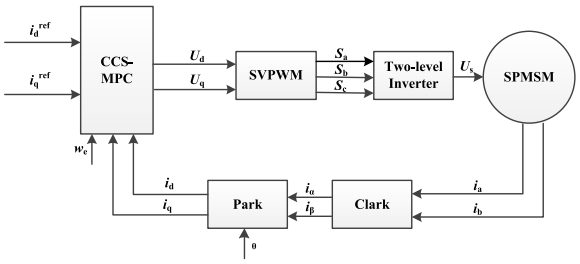

FIGURE 1. The structure diagram of CCS-MPC.

III. MODEL-FREE PREDICTIVE CONTROL

The CCS-MPC method has excellent steady and dynamic performances, but it depends on the mathematical model of SPMSM. The controller performance will be deteriorated if the SPMSM parameters are not measured accurately or the parameters change with the working conditions.

To improve the parameter robustness of the CCS-MPC method, free model current predictive control (FPCC) method which does not use any parameter of SPMSM attracts many researchers' attention. The main idea of FPCC is to use the influence of voltage on current difference for predictive control. The specific implementation steps are shown below.

Assuming the present time is k. First, sampling and storing the stator current $i_{\mathrm{s}}(\mathrm{k})$. Then, calculating the current difference between $i_{\mathrm{s}}(\mathrm{k})$ and $i_{\mathrm{s}}(\mathrm{k}-1)$. Next, storing the current difference as the current difference corresponding to $u(\mathrm{k})$, $u(\mathrm{k})$ represents the voltage vector applied at time k. Finally, predicting the stator current at the next time according to the stored current difference.

In order to improve the prediction accuracy, the current difference will be updated continuously. Due to the sampling period is short enough, the current difference corresponding to the same voltage vector during adjacent periods are considered approximately equal. The flow chart of FPCC method is shown in Figure 2.

Although the FPCC method does not depend on the parameters of SPMSM and has the parameter robustness, but it has the problem of current difference update stagnation. If a voltage vector is not active for several consecutive control periods, the current different corresponding to the voltage vector will stop updating, which may deteriorate the performance of FPCC method. Besides, the FPCC method is only applied to FCS-MPC.

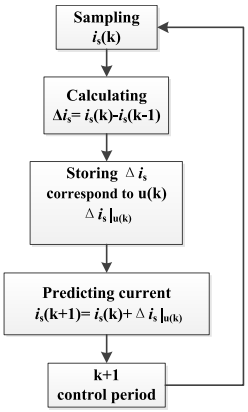

FIGURE 2. The flow chart of FPCC.

This paper proposes an improved FPCC method that can apply to both FCS-MPC and CCS-MPC, and there is no current difference update stagnation problem.

IV. IMPROVED MODEL-FREE PREDICTIVE CONTROL

This paper researches the improved model-free current predictive control method based on CCS-MPC. First, the ultra-local model is described, then introduces the sliding mode observer is introduced into the model, finally, the improved model-free current predictive control method is completely demonstrated.

A. ULTRA-LOCAL MODEL

This paper adopts the single input and single output ultra-local model to substitute the mathematical model of SPMSM. The ultra-local model does not use any motor parameters and takes voltage vector as control variable and the variation of stator current as output variable. The first-order ultra-local model can be described as follow:

$$\dot{y} = F + \alpha u \tag{5}$$

where u denotes control variable and y denotes output variable; α denotes a parameter chosen by the designer; F represents the unknown part of the system.

Substituting the voltage equation of SPMSM into the first-order ultra-local model, the first-order ultra-local model of SPMSM in the rotor rotation coordinate system can be expressed in (6).

$$\begin{aligned} \frac{di_d}{dt} &= F_d + \alpha u_d \\ \frac{di_q}{dt} &= F_q + \alpha u_q \end{aligned} \tag{6}$$

B. SLIDING MODE OBSERVER

To estimate the unknown parameters F_d and F_q, a sliding mode observer (SMO) is selected in this paper.

According to the sliding mode control theory, the sliding mode observer designed process is divided into two steps.

The first step is to determine the sliding surface. The sliding mode state determined by the sliding surface should be asymptotically stable. In this paper, the d-axis current i_d and q-axis current i_q are selected as control variables, and the linear sliding surface s is selected.

$$\begin{aligned} s_d &= \hat{i}_d - i_d \\ s_q &= \hat{i}_q - i_q \end{aligned} \tag{7}$$

The second step is to design the sliding mode control function. The designed sliding mode control function needs to ensure that the sliding mode state reaches the sliding surface in a finite time, and the approaching motion should be as fast as possible with little fluctuation. The exponential approach law is adopted in this paper.

$$\frac{ds}{dt} = -ks - \lambda \text{sign}(s) \tag{8}$$

where k and λ represent slide mode design parameters.

$$\text{sign}(s) = \begin{cases} 1 & s > 0 \\ 0 & s = 0 \\ -1 & s < 0 \end{cases} \tag{9}$$

C. IMPROVED MODEL-FREE PREDICTIVE CURRENT CONTROL

The improved FPCC method does not depend on the parameters of SPMSM and has a better parameter robustness than CCS-MPC. But the ultra-local model of SPMSM has an unknown parameter F, in order to estimate the parameter F, a sliding model observer is designed.

1) CONTROLLER THEORETICAL STUDY

The ultra-local model of SPMSM only contains the designed parameter α and the unknown parameter F. The parameter F includes the parameters of SPMSM essentially, like stator resistance, stator resistance and rotor flux linkage. So the parameter F will also change with the working condition.

Considering the influence of parameter F variation, the extended ultra-local voltage equation of SPMSM can be expressed as:

$$\begin{cases} \dfrac{di_d}{dt} = \alpha u_d + F_d + f_d \\ X_d = F_d + f_d \\ \dfrac{dX_d}{dt} = x_d \end{cases} \tag{10}$$

$$\begin{cases} \dfrac{di_q}{dt} = \alpha u_q + F_q + f_q \\ X_q = F_q + f_q \\ \dfrac{dX_q}{dt} = x_q \end{cases} \tag{11}$$

where f represents the parameter F variation, X represents the sum of parameter F and the variation of parameter F, x is the derivative of X.

To estimate the parameter F, the sliding model observer of SPMSM is designed as follows:

$$\begin{cases} \dfrac{d\hat{i}_{\mathrm{d}}}{dt} = \alpha u_{\mathrm{d}} + \hat{X}_{\mathrm{d}} + U_{\mathrm{dsmo}} \\ \dfrac{d\hat{X}_{\mathrm{d}}}{dt} = \hat{x}_{\mathrm{d}} = g_{\mathrm{d}} U_{\mathrm{dsmo}} \end{cases} \tag{12}$$

$$\begin{cases} \dfrac{d\hat{i}_{\mathrm{q}}}{dt} = \alpha u_{\mathrm{d}} + \hat{X}_{\mathrm{q}} + U_{\mathrm{qsmo}} \\ \dfrac{d\hat{X}_{\mathrm{q}}}{dt} = \hat{x}_{\mathrm{q}} = g_{\mathrm{q}} U_{\mathrm{qsmo}} \end{cases} \tag{13}$$

where $\hat{X}_{\mathrm{d}}$ and $\hat{X}_{\mathrm{q}}$ represent the estimation value of X_{d} and X_{q} respectively, i_{d} and i_{q} denote the estimation currents of d-axis and q-axis respectively, U_{dsmo} and U_{qsmo} denote sliding mode control functions, g_{d} and g_{q} are sliding mode design parameters.

Combining (10), (11), (12), and(13), the current estimation difference equations can be described as follows:

$$\begin{cases} \dfrac{de_1}{dt} = \hat{X}_{\mathrm{d}} - X_{\mathrm{d}} + U_{\mathrm{dsmo}} \\ \dfrac{de_2}{dt} = \hat{X}_{\mathrm{q}} - X_{\mathrm{q}} + U_{\mathrm{qsmo}} \end{cases} \tag{14}$$

$$\begin{cases} \dfrac{de_3}{dt} = g_{\mathrm{d}} U_{\mathrm{dsmo}} - x_{\mathrm{d}} \\ \dfrac{de_4}{dt} = g_{\mathrm{q}} U_{\mathrm{qsmo}} - x_{\mathrm{q}} \end{cases} \tag{15}$$

where $e_1 = \hat{i}_{\mathrm{d}} - i_{\mathrm{d}}$, $e_2 = \hat{i}_{\mathrm{q}} - i_{\mathrm{q}}$, $e_3 = \hat{X}_{\mathrm{d}} - X_{\mathrm{d}}$ and $e_4 = \hat{X}_{\mathrm{q}} - X_{\mathrm{q}}$.

Considering e_3 and e_4 as disturbances and ignoring the influence of the disturbances. The sliding mode control function based on exponential approach law we designed can be described as (16).

$$\begin{aligned} U_{\mathrm{dsmo}} &= -ke_1 - \lambda \mathrm{sign}(e_1) \\ U_{\mathrm{qsmo}} &= -ke_2 - \lambda \mathrm{sign}(e_2) \end{aligned} \tag{16}$$

Substituting the designed sliding mode control function U_{dsmo} and U_{qsmo} into the sliding model observer of (12) and (13). Then use the Euler discretization equation to obtain the current prediction model.

$$\begin{aligned} \hat{i}_{\mathrm{d}}(\mathrm{k}+1) &= i_{\mathrm{d}}(\mathrm{k}) + T_{\mathrm{s}}(\alpha u_{\mathrm{d}} + \hat{X}_{\mathrm{d}} + U_{\mathrm{dsmo}}) \\ \hat{i}_{\mathrm{q}}(\mathrm{k}+1) &= i_{\mathrm{q}}(\mathrm{k}) + T_{\mathrm{s}}(\alpha u_{\mathrm{q}} + \hat{X}_{\mathrm{q}} + U_{\mathrm{qsmo}}) \end{aligned} \tag{17}$$

In order to track the reference current value, make $\hat{i}_{\mathrm{d}}(\mathrm{k}+1)$ equal to $i_{\mathrm{d}}^{\mathrm{ref}}$ and $\hat{i}_{\mathrm{q}}(\mathrm{k}+1)$ equal to $i_{\mathrm{q}}^{\mathrm{ref}}$ directly. Then, the required optimal voltage vectors u_{d} and u_{q} can be obtained.

$$\begin{aligned} u_{\mathrm{d}} &= \frac{1}{\alpha}\left[\frac{i_{\mathrm{d}}^{\mathrm{ref}} - i_{\mathrm{d}}(\mathrm{k})}{T_{\mathrm{s}}} + U_{\mathrm{dsmo}} + \hat{X}_{\mathrm{d}}\right] \\ u_{\mathrm{q}} &= \frac{1}{\alpha}\left[\frac{i_{\mathrm{q}}^{\mathrm{ref}} - i_{\mathrm{q}}(\mathrm{k})}{T_{\mathrm{s}}} + U_{\mathrm{qsmo}} + \hat{X}_{\mathrm{q}}\right] \end{aligned} \tag{18}$$

The system block diagram of improved model-free current predictive control method is showed in Figure 3.

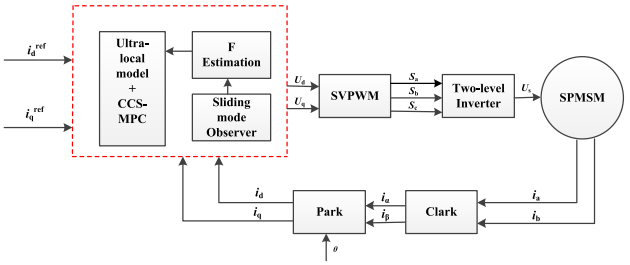

FIGURE 3. The diagram of the improved model-free current predictive control.

The controller designed in this paper has clear concept, simple structure and a small amount of calculation. It is suitable for both FCS-MPC and CCS-MPC and improves the parameter robustness of MPC.

2) CONTROLLER STABILITY ANALYSIS

To prove the designed controller is stable, a positive definite Lyapunov function is selected in this paper.

$$V = \frac{1}{2}s^2 \geq 0 \tag{19}$$

Taking the derivative of V in the (19).

$$\dot{V} = s\dot{s} \tag{20}$$

According to the Lyapunov stability criterion, the designed controller must satisfy the conditions of (21) to make sure the stability of the designed controller.

$$\begin{cases} \dot{V}_{\mathrm{d}} = s_{\mathrm{d}}\dot{s}_{\mathrm{d}} \leq 0 \\ \dot{V}_{\mathrm{q}} = s_{\mathrm{q}}\dot{s}_{\mathrm{q}} \leq 0 \end{cases} \tag{21}$$

Putting $\mathrm{S_d}$ and the derivative of $\mathrm{S_d}$ into the first inequation of (21) to obtain the d-axis stability condition, putting $\mathrm{S_q}$ and the derivative of $\mathrm{S_q}$ into the second inequation of (21) to obtain the q-axis stability condition.

$$\begin{aligned} \dot{V}_{\mathrm{d}} &= s_{\mathrm{d}}\dot{s}_{\mathrm{d}} \\ &= e_1\left(e_3 + U_{\mathrm{dsmo}}\right) \\ &= e_1\left[e_3 - ke_1 - \lambda \mathrm{sign}\left(e_1\right)\right] \\ &= \begin{cases} -ke_1^2 + e_1\left(e_3 - \lambda\right) & e_1 > 0 \\ 0 & e_1 = 0 \\ -ke_1^2 + e_1\left(e_3 + \lambda\right) & e_1 < 0 \end{cases} \end{aligned} \tag{22}$$

$$\begin{aligned} \dot{V}_{\mathrm{q}} &= s_{\mathrm{q}}\dot{s}_{\mathrm{q}} \\ &= e_2\left(e_4 + U_{\mathrm{qsmo}}\right) \\ &= e_2\left[e_4 - ke_2 - \lambda \mathrm{sign}\left(e_4\right)\right] \\ &= \begin{cases} -ke_2^2 + e_2\left(e_4 - \lambda\right) & e_4 > 0 \\ 0 & e_4 = 0 \\ -ke_2^2 + e_2\left(e_4 + \lambda\right) & e_4 < 0 \end{cases} \end{aligned} \tag{23}$$

Making sure the designed controller satisfy the stability conditions, the parameter k and parameter λ should be satisfied the (24).

$$\begin{cases} \lambda > max\left(|e_3|, |e_4|\right) \\ k \geq 0 \end{cases} \tag{24}$$

To make sure e_3, e_4 and their derivative converge to zero asymptotically, they must also meet the stability criteria of Lyapunov.

$$\begin{cases} \dot{e}_3 + x_\mathrm{d} + g_\mathrm{d}(ke_3 + \lambda \mathrm{sign}(e_3)) = 0 \\ \dot{e}_4 + x_\mathrm{q} + g_\mathrm{q}(ke_4 + \lambda \mathrm{sign}(e_4)) = 0 \end{cases} \tag{25}$$

Solving the above equations, we can obtain the solutions of e_3 and e_4.

$$\begin{cases} e_3 = e^{-g_\mathrm{d}kt}[C + \int (x_\mathrm{d} + A)e^{g_\mathrm{d}kt}] \\ e_4 = e^{-g_\mathrm{q}kt}[C + \int (x_\mathrm{q} + A)e^{g_\mathrm{q}kt}] \end{cases} \tag{26}$$

where C and A are constant, in order to make e_3 and e_4 converge to zero, $\mathrm{g_d}$ and $\mathrm{g_q}$ should be positive values.

The above proof process prove the proposed control method is stable under appropriate parameter design.

V. SIMULATION STUDY

In order to verify the effectiveness of the improved model-free predictive control method, the CCS-MPC method and the improved FPCC method are testified in the Matlab/Simulink environment. This paper compares the simulation results of the two methods under steady state, dynamic state and parameters mismatch conditions. The simulation results are showed in the figures below.

The research object of this paper is surface-mounted permanent magnet synchronous motor (SPMSM). Table 1 lists the actual parameters of SPMSM used in the simulation and experiment. The sampling period is 50us and the parameters of sliding model observer are designed as $k_1 = 0.1$, $\lambda = 12000$, $g_\mathrm{d} = 800$, $g_\mathrm{q} = 800$, the parameter of ultra-local model is designed as $\alpha = 820$.

TABLE 1. SPMSM parameters.

Parameter	Value	Unit
Number of pole pairs p	4	\
Stator resistance R_s	0.365	Ω
Stator inductance L_s	1.225	mH
Rotor magnet flux Ψ_f	0.1667	wb
Rotational inertia J	0.00194	kg · m^2
Rated power P_N	2.6	kW
Rated torque T_N	10	Nm

First, Simulation model is built in Matlab/Simulink environment and the steady-state performance of the two methods are tested. The steady-state simulation conditions are that the speed is 500r/min, the load torque is 8 Nm, and initial inductance is 2 times mismatch $L_\mathrm{s}' = 2\,L_\mathrm{s}$.

Figure 4 shows the steady-state simulation results of the two methods. From the simulation results we can see that the

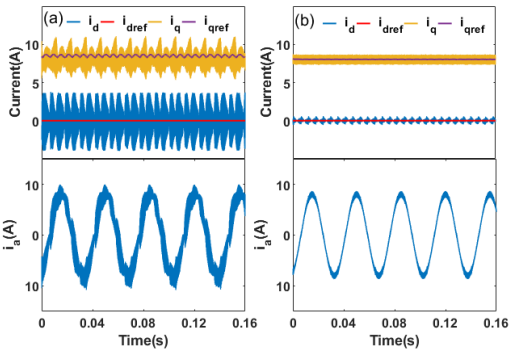

FIGURE 4. Simulation results under steady state (a) CCS-MPC method (b) Improved FPCC method.

current harmonic content of CCS-MPC method is large than the proposed method. To verify the result further, the quantitative calculation is carried out, the A-phase current total harmonic distortion (THD) of CCS-MPC method is 57.23%, and the THD of the proposed method is 19.42%, which is much lower than CCS-MPC method.

Second, for the sake of proving the improved FPCC method has the capability of suppressing parameters disturbance, a series of dynamic simulation tests are carried out under parameter mismatch conditions.

The first group of dynamic simulation conditions are stator inductance mismatch $L_\mathrm{S}' = 2L_\mathrm{S}$, the load torque steps to 10Nm from 2Nm at 0.05s and drops to 5Nm at 0.1s. The speed of Figure 5 is 300 r/min, the speed of Figure 6 is 1000r/min.

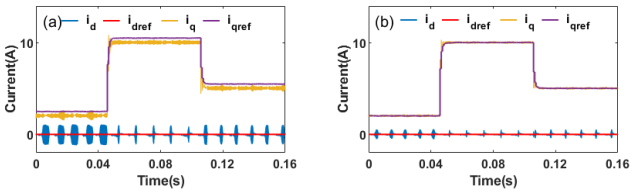

FIGURE 5. Simulation results under inductance mismatch at 300r/min (a) CCS-MPC method (b) Improved FPCC method.

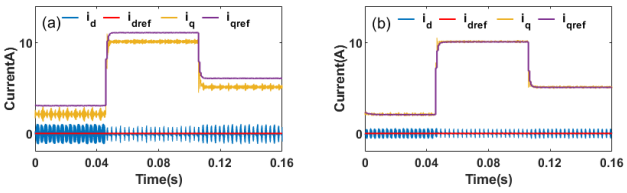

FIGURE 6. Simulation results under inductance mismatch at 1000r/min (a) CCS-MPC method (b) Improved FPCC method.

It can be seen that the dq axis current harmonic content of CCS-MPC method is larger than the proposed method, and the q-axis current following characteristic is worse than the improved FPCC method. Simulation results show that the improved FPCC has strong robustness to inductance mismatch.

The second group of dynamic simulation conditions are flux linkage mismatch, the load torque steps to 6Nm from 2Nm at 0.05s and then reduces to 4Nm at 0.1s. The flux linkage mismatch of Figure 7 is $\psi_f' = 0.8\psi_f$ and the speed is 300r/min, the flux linkage mismatch of Figure 8 is $\psi_f' = 1.4\psi$ and the speed is 1000r/min.

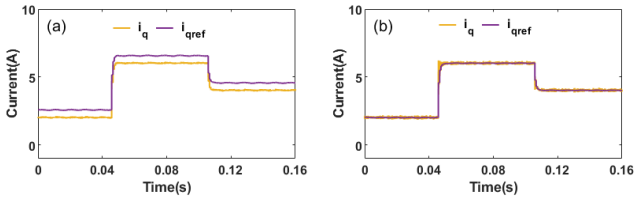

FIGURE 7. Simulation results under flux linkage mismatch at 300r/min (a) CCS-MPC method (b) Improved FPCC method.

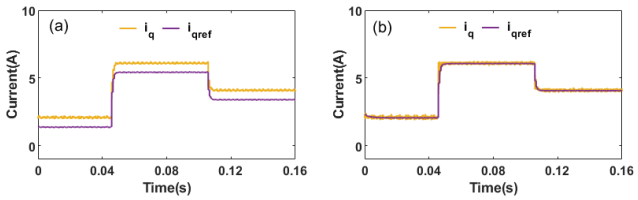

FIGURE 8. Simulation results under flux linkage mismatch at 1000r/min (a) CCS-MPC method (b) Improved FPCC method.

The simulation results show that the q-axis current of the improved FPCC method can accurately track the reference current value when the flux linkage disturbance appear, whatever in low speed or in the high speed. While the q-axis current of the CCS-MPC method has a poor following characteristic. This indicates the proposed control method has good robustness in the case of flux linkage mismatch.

The third group of dynamic simulation conditions are resistance mismatch, the load torque steps from 2Nm to 6Nm at 0.05s, then reduces to 4Nm at 0.1s. The resistance mismatch of Figure 9 is $R_S' = 15R_S$ and the speed is 1000r/min, the resistance mismatch of Figure 10 is $R_S' = 0.1R_S$ and the speed is 300r/min.

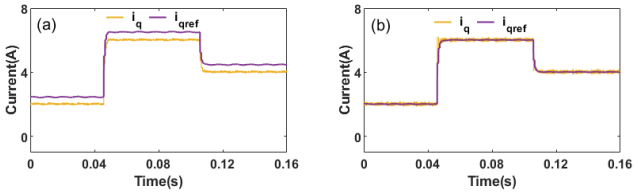

FIGURE 9. Simulation results under resistance mismatch at 300r/min (a) CCS-MPC method (b) Improved FPCC method.

From Figure 9 and Figure 10, the q-axis current of the improved FPCC method can accurately track the reference current value, while the q-axis current of CCS-MPC method has a certain difference from the reference current. This shows the proposed control method has good robustness in the case of resistance mismatch.

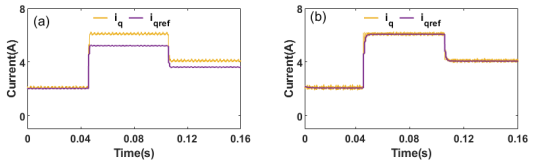

FIGURE 10. Simulation results under resistance mismatch at 1000r/min (a) CCS-MPC method (b) Improved FPCC method.

To further verify the parameter robustness of the proposed improved FPCC method, the forth group of simulation conditions are inductance mismatch, resistance mismatch and flux linkage mismatch at the same time. The conditions of Figure 11 are inductance mismatch $L_s' = 1.8L_s$, resistance mismatch $R_s' = 0.1R_s$ and flux linkage mismatch $\psi_f' = 0.5\psi_f$, the speed is 800 r/min, the load torque steps from 2Nm to 8Nm at 0.05s, and then drops to 4Nm at 0.1s. The conditions of Figure 12 are inductance mismatch $L_s' = 1.5L_s$, resistance mismatch $R_s' = 10R_s$ and flux linkage mismatch $\psi_f' = 1.5\ \psi_f$, the speed is 900 r/min, the load torque steps to 7Nm from 2Nm at 0.05s, then reduces to 3Nm at 0.1s.

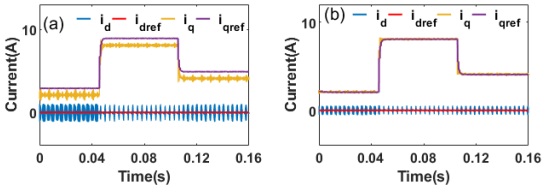

FIGURE 11. Simulation results under $L_s' = 1.8\ L_s$, $R_s' = 0.1\ R_s$, $\psi_f' = 0.5\ \psi_f$ condition (a) CCS-MPC method (b) Improved FPCC method.

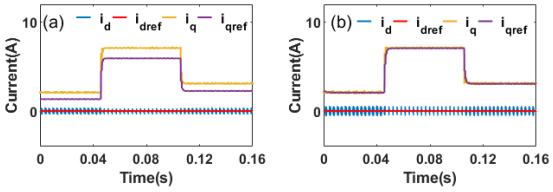

FIGURE 12. Simulation results under $L_s' = 1.5\ L_s$, $R_s' = 10\ R_s$, $\psi_f' = 1.5\ \psi_f$ condition (a) CCS-MPC method (b) Improved FPCC method.

From Figure 11 and Figure 12, when the stator resistance, stator inductance and rotor flux linkage mismatch at the same time, the q-axis current of the improved FPCC method still has a good following characteristic. That means the improved FPCC method has the ability to suppress multiparameter disturbance.

The above simulation results verify the proposed method has strong parameter robustness.

VI. EXPERIMENTAL RESULTS

To verify the real control effect of the improved FPCC method, two control methods, CCS-MPC method and improved FPCC method are applied to the actual motor control system. The experimental platform of SPMSM is shown in Figure 13, which mainly includes a drive motor, a load motor, an oscilloscope, a torque analyzer, a power supply, an emulator and a computer. The chip of controller is

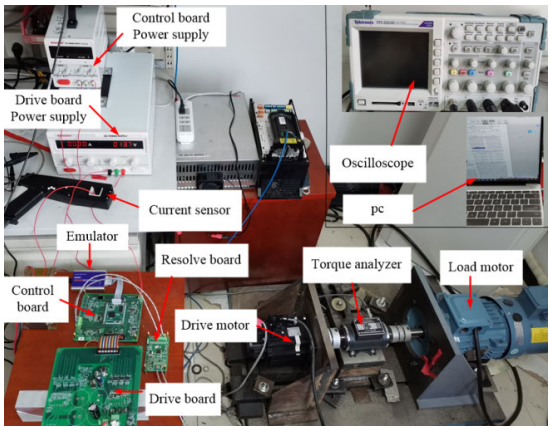

FIGURE 13. Experimental platform of SPMSM drive system.

DSP-TMS320F28377d, the sampling frequency is 20kHz and the bus voltage is set to 150v.

The working condition of the experiments is designed to be similar to the simulation tests. First, the steady-state working conditions are designed. The speed is 500r/min, the load torque is 8 Nm and the initial inductance is 2 times mismatch $L_s' = 2\,L_s$. The current characteristics of the two methods are presented in Figure 14. To quantitatively describe the current characteristic, the THD of stator current is calculated based on the experimental data. The THD of CCS-MPC method is 63.35% and the THD of the improved FPCC method is 53.77%. The current characteristic and the calculation results show that the improved FPCC method can effectively reduce the harmonic content of stator current.

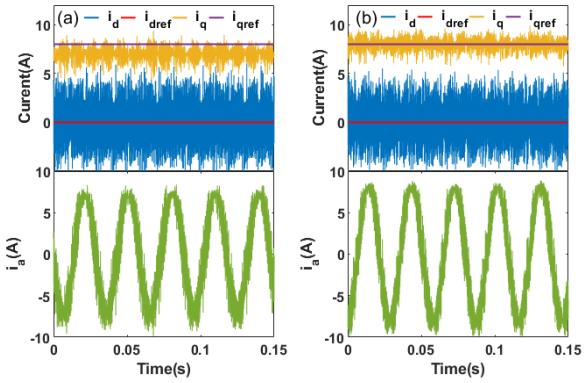

FIGURE 14. Experimental results under steady state (a) CCS-MPC method (b) Improved FPCC method.

Second, to verify that the proposed method has parameter robustness, experimental tests are carried out under different parameter mismatch conditions.

Figure 15 shows the experimental results of i_d and i_q in the conditions of the inductance mismatch is $L_s' = 3L_s$, the speed is 1000r/min and the load torque steps to 10Nm from 2Nm at 0.05s and then reduces to 5Nm at 0.1s.

From the experimental results, the ripple of q-axis current i_q of CCS-MPC method is obviously larger than the improved FPCC method. Besides, the improved

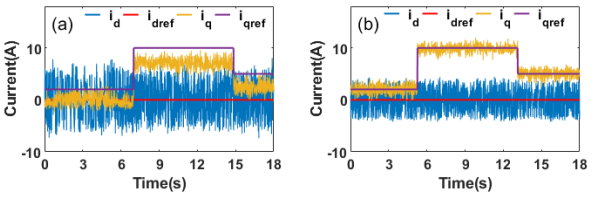

FIGURE 15. Experimental results under inductance mismatch at 1000r/min (a) CCS-MPC method (b) Improved FPCC method.

FPCC method can track the reference current value accurately, while CCS-MPC method has the following error, which shows that the improved FPCC method has the ability to effectively suppress inductance disturbance.

Figure 16 shows the experimental results of i_q in the conditions of the flux linkage mismatch is $\psi_f' = 3\psi_f$, the speed is 300r/min. Figure 17 shows the experimental results of i_q in the conditions of the flux linkage mismatch is $\psi_f' = 0.3\psi_f$, the speed is 1000r/min. The load torque steps from 2Nm to 6Nm at 0.05s, then reduces to 4Nm at 0.1s.

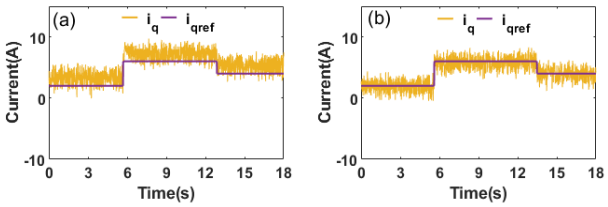

FIGURE 16. Experimental results under flux linkage mismatch at 300r/min (a) CCS-MPC method (b) Improved FPCC method.

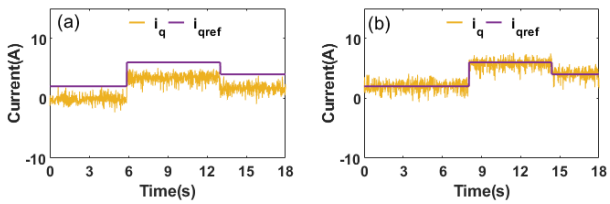

FIGURE 17. Experimental results under flux linkage mismatch at 1000r/min (a) CCS-MPC method (b) Improved FPCC method.

The experimental results are consistent with the simulation results, the q-axis current following characteristics of the improved FPCC method are better than CCS-MPC method, which indicates that the improved FPCC method can effectively suppress flux linkage disturbance.

Figure 18 shows the experimental results of i_q in the conditions of the resistance mismatch is $R_s' = 15R_s$, the speed is 300r/min. Figure 19 shows the experimental results of i_q in the conditions of the resistance mismatch is $R_s' = 0.1R_s$, the speed is 1000r/min. The load torque steps from 2Nm to 6Nm at 0.05s, then drops to 4Nm at 0.1s.

Figure 18 and Figure 19 indicate that the q-axis current of the improved FPCC method can accurately follow the reference current value in the case of resistance mismatch, while the q-axis current of CCS-MPC method has

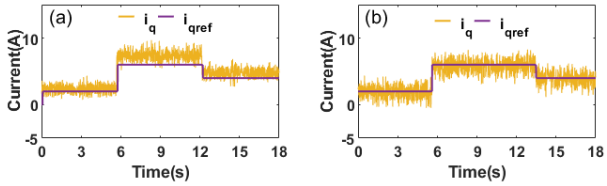

FIGURE 18. Experimental results under resistance mismatch at 300r/min (a) CCS-MPC method (b) Improved FPCC method.

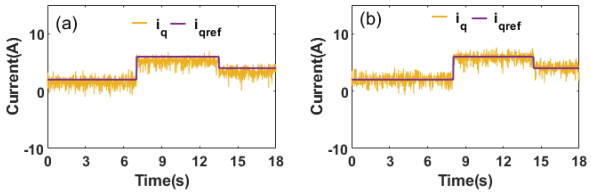

FIGURE 19. Experimental results under resistance mismatch at 1000r/min (a) CCS-MPC method (b) Improved FPCC method.

a following error. Which shows that the improved FPCC method can effectively suppress resistance disturbance.

Similarly, to further verify the parameter robustness of the improved FPCC method, experimental tests are carried out in the condition of multiparameter mismatch.

The working conditions of Figure 20 are that the inductance mismatch is $L_s' = 2L_s$, the resistance mismatch is $R_s' = 0.1R_s$ and the flux linkage mismatch is $\psi_f' = 0.5\ \psi_f$, the speed is 800 r/min, and the load torque steps from 2Nm to 8Nm at 0.05s, then reduces to 4Nm at 0.1s. The working conditions of Figure 21 are that the inductance mismatch is $L_s' = 1.5L_s$, the resistance mismatch is $R_s' = 10R_s$ and the flux linkage mismatch is $\psi_f' = 2\psi_f$, the speed is 900 r/min, and the load torque steps from 2Nm to 7Nm at 0.05s, then reduces to 3Nm at 0.1s.

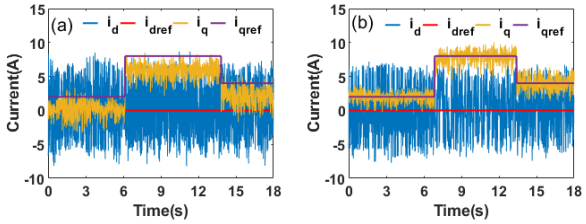

FIGURE 20. Experimental results under multi-parameters mismatch at 800r/min (a) CCS-MPC method (b) Improved FPCC method.

It can be seen from the experimental results that the q-axis current of the improved FPCC method can track the reference current accurately, and has strong parameter robustness in the case of multi-parameters mismatch.

According to the above experimental results, it can be concluded that the proposed method can effectively suppress the inductance disturbance, resistance disturbance and flux linkage disturbance in various working conditions, so it has strong parameter robustness.

To compare the current fluctuation of CCS-MPC method and improved FPCC method more intuitively, Table 2 lists

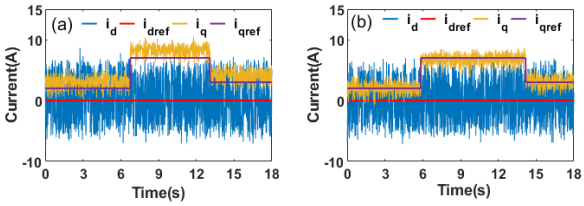

FIGURE 21. Experimental results under multi-parameters mismatch at 900r/min (a) CCS-MPC method (b) Improved FPCC method.

TABLE 2. THD(%) of two methods under $L_s' = 2L_s$ situation.

Speed(r/min)	CCS-MPC	Improved FPCC
400	46.61	38.40
500	44.94	38.24
600	42.43	34.27
700	53.64	40.40
800	52.54	37.54
900	64.40	44.11
1000	66.08	45.53

the THD of phase current i_a of two methods with $L_s' = 2L_s$ at different speeds.

VII. CONCLUSION

To enhance the parameter robustness of MPC method and improve the predictive performance of MPC method, an improved free-model predictive control method is proposed in this paper. The conclusions of this paper are as follows.

1) The model-free predictive control method based on SPMSM ultra-local model does not need any motor parameters.
2) The structure of the designed sliding mode observer is simple, improving the current prediction accuracy and reducing the calculation burden of the control system.
3) Simulation and experimental results show that the proposed method has the ability to suppress parameters disturbance and has strong parameter robustness.

REFERENCES

[1] Z. Q. Zhu and D. Howe, "Electrical machines and drives for electric, hybrid, and fuel cell vehicles," *Proc. IEEE*, vol. 95, no. 4, pp. 746–765, Apr. 2007.
[2] D. Casadei, F. Profumo, G. Serra, and A. Tani, "FOC and DTC: Two viable schemes for induction motors torque control," *IEEE Trans. Power Electron.*, vol. 17, no. 5, pp. 779–787, Sep. 2002.
[3] Y. Zhang and J. Zhu, "Direct torque control of permanent magnet synchronous motor with reduced torque ripple and commutation frequency," *IEEE Trans. Power Electron.*, vol. 26, no. 6, pp. 235–248, Jan. 2011.
[4] L. Zhong, M. F. Rahman, W. Y. Hu, and K. W. Lim, "Analysis of direct torque control in permanent magnet synchronous motor drives," *IEEE Trans. Power Electron.*, vol. 12, no. 3, pp. 528–536, May 1997.

[5] Y. Zhang, D. Xu, J. Liu, S. Gao, and W. Xu, "Performance improvement of model-predictive current control of permanent magnet synchronous motor drives," *IEEE Trans. Ind. Appl.*, vol. 53, no. 4, pp. 3683–3695, Jul./Aug. 2017.

[6] M. Preindl and S. Bolognani, "Comparison of direct and PWM model predictive control for power electronic and drive systems," in *Proc. 28th Annu. Appl. Power Electron. Conf. Expo. (APEC)*, Mar. 2013, pp. 2526–2533.

[7] P. Cortes, M. P. Kazmierkowski, R. M. Kennel, D. E. Quevedo, and J. Rodriguez, "Predictive control in power electronics and drives," *IEEE Trans. Ind. Electron.*, vol. 55, no. 12, pp. 4312–4324, Dec. 2008.

[8] J. Rodriguez, J. Pontt, C. Silva, P. Correa, P. L. Illesca, P. Cortes, and U. Ammann, "Predictive current control of a voltage source inverter," *IEEE Trans. Ind. Electron.*, vol. 54, no. 1, pp. 495–503, Mar. 2007.

[9] S. Vazquez, J. I. Leon, L. G. Franquelo, and J. Rodriguez, "Model predictive control: A review of its applications in power electronics," *IEEE Ind. Electron. Mag.*, vol. 8, no. 1, pp. 16–31, Mar. 2014.

[10] R. Errouissi, M. Ouhrouche, W.-H. Chen, and A. M. Trzynadlowski, "Robust cascaded nonlinear predictive control of a permanent magnet synchronous motor with antiwindup compensator," *IEEE Trans. Ind. Electron.*, vol. 59, no. 8, pp. 3078–3088, Aug. 2012.

[11] P. Wipasuramonton, Z. Q. Zhu, and D. Howe, "Predictive current control with current-error correction for PM brushless AC drives," *IEEE Trans. Ind. Appl.*, vol. 42, no. 4, pp. 1071–1079, Aug. 2006.

[12] Y. A.-R.-I. Mohamed and E. F. El-Saadany, "Robust high bandwidth discrete-time predictive current control with predictive internal model—A unified approach for voltage-source PWM converters," *IEEE Trans. Power Electron.*, vol. 23, no. 1, pp. 126–136, Jan. 2008.

[13] J. Yu, P. Shi, W. Dong, B. Chen, and C. Lin, "Neural network-based adaptive dynamic surface control for permanent magnet synchronous motors," *IEEE Trans. Neural Netw. Learn. Syst.*, vol. 26, no. 3, pp. 640–645, Mar. 2015.

[14] S. J. Jeong and S. H. Song, "Improvement of predictive current control performance using online parameter estimation in phase controlled rectifier," *IEEE Trans. Power Electron.*, vol. 22, no. 5, pp. 1820–1825, Sep. 2007.

[15] J. Yang, W.-H. Chen, S. Li, L. Guo, and Y. Yan, "Disturbance/uncertainty estimation and attenuation techniques in PMSM drives—A survey," *IEEE Trans. Ind. Electron.*, vol. 64, no. 4, pp. 3273–3285, Apr. 2017.

[16] X. Zhang, B. Hou, and Y. Mei, "Deadbeat predictive current control of permanent-magnet synchronous motors with stator current and disturbance observer," *IEEE Trans. Power Electron.*, vol. 32, no. 5, pp. 3818–3834, May 2017.

[17] X. Li, S. Zhang, C. Zhang, Y. Zhou, and C. Zhang, "An improved deadbeat predictive current control scheme for open-winding permanent magnet synchronous motors drives with disturbance observer," *IEEE Trans. Power Electron.*, vol. 36, no. 4, pp. 4622–4632, Apr. 2021.

[18] L. Yan and X. Song, "Design and implementation of Luenberger model-based predictive torque control of induction machine for robustness improvement," *IEEE Trans. Power Electron.*, vol. 35, no. 3, pp. 2257–2262, Mar. 2020.

[19] M. Fliess and C. Join, "Model-free control and intelligent pid controllers: Towards a possible trivialization of nonlinear control?" *IFAC Proc. Volumes*, vol. 42, no. 10, pp. 1531–1550, 2009.

[20] Y. Chen, T.-H. Liu, C.-F. Hsiao, and C.-K. Lin, "Implementation of adaptive inverse controller for an interior permanent magnet synchronous motor adjustable speed drive system based on predictive current control," *IET Electr. Power Appl.*, vol. 9, no. 1, pp. 60–70, 2015.

[21] C.-K. Lin, T.-H. Liu, J.-T. Yu, L.-C. Fu, and C.-F. Hsiao, "Model-free predictive current control for interior permanent-magnet synchronous motor drives based on current difference detection technique," *IEEE Trans. Ind. Electron.*, vol. 61, no. 2, pp. 667–681, Feb. 2014.

[22] C.-K. Lin, J.-T. Yu, Y.-S. Lai, and H.-C. Yu, "Improved model-free predictive current control for synchronous reluctance motor drives," *IEEE Trans. Ind. Electron.*, vol. 63, no. 6, pp. 3942–3953, Jun. 2016.

[23] Y. Zhou, H. Li, and H. Zhang, "Model-free deadbeat predictive current control of a surface-mounted permanent magnet synchronous motor drive system," *J. Power Electron.*, vol. 18, no. 1, pp. 103–115, Jan. 2018.

[24] Y. Zhou, H. Li, and H. Yao, "Model-free control of surface mounted PMSM drive system," in *Proc. IEEE Int. Conf. Ind. Technol. (ICIT)*, Taipei, Taiwan, Mar. 2016, pp. 175–180.

[25] Y. Zhang, J. Jin, and L. Huang, "Model-free predictive current control of PMSM drives based on extended state observer using ultralocal model," *IEEE Trans. Ind. Electron.*, vol. 68, no. 2, pp. 993–1003, Feb. 2021.

XUERONG LI received the B.Eng. degree in vehicle engineering from Qingdao University, in 2019. She is currently pursuing the M.Sc. degree with the National Engineering Laboratory for Electric Vehicles, School of Mechanical Engineering, Beijing Institute of Technology. Her research interests include predictive control for synchronous motor drive and phase current reconstruction.

YANG WANG received the Ph.D. degree in mechanical engineering from Beijing Institute of Technology, in June 2016. In 2016, he joined as a Research Assistant with China North Vehicle Research Institute, where he currently holds the Discipline Leader and a Senior Research Fellow positions. His current research interests include optimal and adaptive control, intelligent control, motion planning, and control problems related to unmanned aerial/ground vehicles.

XINGZHONG GUO is currently the President, a Professor, a Tutor, and an academic backbone of Anhui Polytechnic University. He has long engaged in power electronics and electric transmission, intelligent control theory, system modeling and simulation, and automation research. The intelligent control, system modeling and simulation, and electric transmission has accumulated relatively rich experience in his research and teaching. In recent years, he has published dozens of academic articles, four of which were included in EI.

XING CUI received the Ph.D. degree in vehicle engineering from Beijing Institute of Technology, Beijing, China, in 2007.

He is currently a Senior Research Fellow with China North Vehicle Research Institute, China North Industries Group Corporation (NORINCO). His research interests include unmanned ground vehicle design, multi-motor driving systems, distributing drive and control systems, and system integration.

SHUO ZHANG (Member, IEEE) received the B.Eng. degree from North China Institute of Aerospace Engineering, Hebei, China, in 2011, and the Ph.D. degree in vehicle engineering from Beijing Institute of Technology, Beijing, China, in 2017.

He is currently an Assistant Professor with the National Engineering Laboratory for Electric Vehicles, School of Mechanical Engineering, Beijing Institute of Technology. His research interests include the modeling and control for the permanent magnet synchronous motor, multi-motor driving systems, and hybrid power systems.

YONGSHEN LI (Graduate Student Member, IEEE) was born in Liaoning, China, in 1998. He received the B.Eng. degree in vehicle engineering from Beijing Institute of Technology, Beijing, China, in 2019, where he is currently pursuing the M.Sc. degree with the National Engineering Laboratory for Electric Vehicles, School of Mechanical Engineering.

His research interests include predictive control for synchronous motor drive and multi-phase motor drives.